Mutagenesis Advance Access published August 11, 2010
Mutagenesis pp. 1–6, 2010 doi:10.1093/mutage/geq044

Mutational analysis of *RUNX2* gene in Chinese patients with cleidocranial dysplasia

Chenying Zhang, Shuguo Zheng*, Yixiang Wang[1], Yuming Zhao, Junxia Zhu and Lihong Ge

Department of Pediatric Dentistry and [1]Research Laboratory of Oral and Maxillofacial Surgery, Peking University School and Hospital of Stomatology, 22 Zhongguancun Nandajie, Haidian District, Beijing 100081, China.

*To whom correspondence should be addressed. Department of Pediatric Dentistry, Peking University School and Hospital of Stomatology, 22 Zhongguancun Nandajie, Haidian District, Beijing 100081, China. Tel: +86 10 62179977 5361; Fax: +86 10 62173402; Email: zhengsg86@gmail.com

Received on March 26, 2010; revised on June 19, 2010; accepted on July 15, 2010

Cleidocranial dysplasia (CCD) is a dominantly inherited skeletal dysplasia caused by mutations in the osteoblast-specific transcription factor-encoding gene, *RUNX2*. To correlate different *RUNX2* mutations with CCD clinical spectrum, we studied six independent Chinese CCD patients. In five patients, mutations were detected in the coding region of the *RUNX2* gene, including two frameshift mutations and three missense mutations. Of these mutations, four were novel and one had previously been reported. All the detected mutations were exclusively clustered within the Runt domain that affected conserved residues in the Runt domain. *In vitro* green fluorescent protein fusion studies showed that the three mutations—R225L, 214fs and 172fs—interfered with nuclear accumulation of RUNX2 protein, while T200I mutation had no effect on the subcellular distribution of RUNX2. There was no marked phenotypic difference between patients in craniofacial and clavicles features, while the expressivity of supernumerary teeth in our patient cohort had a striking variation, even among family members. The occurrence of intrafamilial clinical variability raises the view that hypomorphic effects and genetic modifiers may alter the clinical expressivity of these mutations. Our results provide new genetic evidence that mutations involved in *RUNX2* contribute to CCD.

Introduction

Cleidocranial dysplasia (CCD; MIM 119600) is a dominantly inherited autosomal bone disease that is characterised by persistently open sutures or delayed closure of sutures, hypoplastic or aplastic clavicles, short stature, supernumerary teeth, delayed eruption of permanent dentition and other skeletal anomalies (1). The common craniofacial features of this disease include brachycephaly, delayed closure of the fontanelles and sutures, wormian bones, frontal and biparietal bossing, relative macrocephaly, depressed nasal bridge and midface hypoplasia. Dental anomalies and some degrees of clavicular hypoplasia seem to be consistent features of the disorder (2,3). However, the phenotypic spectrum in different individuals varies dramatically, even within families, ranging from mildly affected individuals with only dental abnormalities to severely affected individuals with severe osteoporosis (2).

Mutations in the *runt*-related transcription factor 2 gene (*RUNX2*, also known as *CBFA1*, *PEBP2aA* and *AML3*) located on chromosome 6p21 have been identified as the cause of CCD (4,5). *RUNX2* is required for mesenchymal condensation, osteoblast differentiation from mesenchymal stem cells, chondrocyte hypertrophy and vascular invasion of developing skeletons (6,7). *RUNX2* homozygous mice completely lack osteoblasts and bone and die of respiratory failure shortly after birth; heterozygous *RUNX2* mutant mice display all the hallmarks of CCD, including open fontanelles and hypoplastic clavicles, but not the dental anomalies (6,8).

RUNX2 encodes a transcription factor that belongs to the core-binding factor α family. It is homologous to the *Drosophila* pair-rule gene *runt* and is characterised by the 128 amino acids long evolutionary conserved Runt domain. Runt domain is responsible for DNA binding and heterodimerisation with a non DNA-binding core-binding factor β (CBFβ) subunit (9). And the resulting complex binds to *cis*-acting elements and regulates skeletal formation-related genes, such as *osteocalcin*, expression (10). The Runt domain also contains a nuclear-localisation signal (NLS) that is essential for accumulation of RUNX2 protein in the nucleus (2). The C-terminus of RUNX2 is a region rich in proline, serine and threonine (PST domain), which are necessary for RUNX2-mediated transcriptional regulation and are involved in functional interactions with various other transcription factors, coactivators and corepressors (11,12).

Up to the present, numerous mutations in *RUNX2* have been identified in patients with CCD (13–16). Most of the missense mutations were located in the Runt domain involving heterodimerisation and DNA binding with CBFβ (17,18). Nonsense, splicing mutation and insertion/deletions were also found and they were scattered throughout the entire *RUNX2* gene.

In this study, we have performed screening and functional analysis of *RUNX2* mutations in six Chinese patients with the clinical diagnosis of CCD. The purpose of this study was to identify the spectrum of mutations in *RUNX2* in this population and to analyse the genotype–phenotype correlations accordingly and then assessed subcellular localisation of the RUNX2 mutants.

Materials and methods

Patients

Six unrelated families with the clinical diagnosis of CCD [for review of diagnostic criteria, see Mundlos (1)] were investigated in the present study. Informed consent was obtained from all individuals. All the study protocols were approved by the Ethical Committee of Peking University Heath Science Center (approval number: IRB00001052-07100).

Mutation analysis

Genomic DNA was extracted from the peripheral blood of the patients by using a TIANamp Blood DNA mini kit (TIANGEN, Beijing, China) according to the

© The Author 2010. Published by Oxford University Press on behalf of the UK Environmental Mutagen Society.
All rights reserved. For permissions, please e-mail: journals.permissions@oxfordjournals.org.

Downloaded from mutage.oxfordjournals.org at Peking University on September 26, 2010

manufacturer's instruction. The entire coding region of the *RUNX2* gene (from exon 1 to exon 8) was amplified by polymerase chain reaction (PCR) using the intron–exon specific primers as described previously [Quack *et al.* (2)]. In a DNA Engine PTC-200, 35 cycles of PCR were preceded by an initial denaturation at 94°C for 5 min, denaturation 94°C for 20 sec, annealing at 62°C for 30 sec and extension at 72°C for 1 min, followed with a 7-min extension at 72°C. For exon 1, dimethyl sulphoxide (DMSO) was added at a final concentration of 10% and for exon 7, 5% DMSO was added. The amplification products were checked by 2% agarose gel electrophoresis and purified with the PCR purification kit (Omega, Norcross, GA, USA) according to manufacturer's instructions. Purified PCR products were sequenced using an ABI 3730 XL automatic sequencer (ABI, Foster City, CA, USA). DNA sequences were analysed using all the databases of NCBI and the BLASTN (BLAST nucleotide) program (http://blast.ncbi.nlm.nih.gov/). The exons are numbered according to GenBank entries AF001443–AF001450. Each mutation was confirmed in at least two independent experiments by nucleotide sequencing.

Design of expression vectors, cloning and mutagenesis

In order to transiently express green fluorescent protein fusions, full-length *RUNX2* complementary DNA had been amplified from pCMV5-RUNX2 plasmid (a generous gift from Dr Renny T. Franceschi, School of Dentistry, University of Michigan) by PCR using forward (5′-TCAGATCTATGGCGT-CAAACAGCCTCTTCAGCGC-3′) and reverse (5′-GGCGTCGACTGA-TATGGCCGCCAAACAGACTC-3′) primers containing BglII and SalI sites, respectively. Then, the resulting open reading frame was subcloned into BglII/SalI sites of the pEGFP-N1 vector (a generous gift of Dr Y. H. Gan, Research Laboratory of Oral and Maxillofacial Surgery, Peking University School and Hospital of Stomatology). The construct was completely sequenced to exclude random mutagenesis and was used as template for all other subcloning strategies. The mutants carrying T200I, R225L and 214fs mutations were constructed, respectively, using the QuikChange Lightning Site-Directed Mutagenesis Kit (Stratagene, La Jolla, CA, USA) following the manufacturer's instructions. All plasmids were fully sequenced in order to confirm the target mutations and exclude any additional mutations.

Cell culture and transient transfection

The human embryonic kidney (HEK) 293A cells (a generous gift of Dr T. J. Li, Department of oral Pathology, Peking University School and Hospital of Stomatology) were cultured at 37°C and under a 5% CO_2 atmosphere in Dulbecco's modified Eagle's medium (Gibco, Gaithersburg, MD, USA) supplemented with 10% foetal bovine serum (FBS) (Gibco), 100 U/ml penicillin and 100 mg/ml streptomycin.

For transient transfection, 293A cells were trypsinised, counted and plated onto a glass coverslip in a six-well plate at a cell density of 2.5×10^5 per well. After overnight incubation, 2 μg of plasmid DNA was transfected into cells using 2 μl of Lipofectamine 2000 (Invitrogen, Carlsbad, USA, CA) following the manufacturer's instruction. Six hours after transfection, serum-free medium was replaced by fresh growth medium with 10% FBS. Duplicate slides were seeded for each transfection, and the results were observed under confocal microscope after 48 h past transfection.

Microscopic examination of cells

Transfected 293A cells were fixed with 4% paraformaldehyde in phosphate-buffered saline (PBS) for 10 min at room temperature and washed three times with PBS. Cell nuclei were visualised by stained with 4′,6-diamidino-2-phenylindole (DAPI; Sigma, St Louis, MO, USA) at a concentration of 2 μg/ml for 20 min, followed by destaining with PBS for 20 min. Coverslips were mounted with Vectashield (Vector Laboratories) and examined with a Leica TCS SP5 confocal microscopy (Leica Microsystems, Heidelberg, Germany).

Results

Clinical data

Six unrelated Chinese families with clinical diagnosis of CCD were included in the present study (Table I). Among them, three families were familial cases and the remainders were sporadic ones. All the patients showed classic CCD phenotypes: hypoplastic clavicles and delayed closure of the anterior fontanelle in addition to the observation of classic craniofacial features. In addition, dental anomalies including retained deciduous teeth and delayed eruption of permanent teeth were also observed in all patients, though no supernumerary teeth exist in two familial cases. However, stature was found to be significantly reduced only in male patients with CCD.

Mutation analysis and phenotypic correlations

To identify mutations in *RUNX2* gene in CCD patients, we analysed the coding region of the *RUNX2* gene. The DNA fragments from exon 1 to exon 8 of *RUNX2* were amplified by genomic PCR and directly sequenced. By this approach, five different types of heterozygous mutations and an additional polymorphism were identified in five probands and summarised in Table I and supplementary Figure S1, available at *Mutagenesis* Online, and the detection of parts of the mutations had been reported in our previous report (19). However, there was no mutation detected in one familial case. Of these identified mutations, four were novel and one was reported before.

Missense mutations

In our patient cohort, three missense mutations were detected in three probands. Two (c.599C>T, p.Thr200Ile and c.674G>T, p.Arg225Leu) were novel, and the other (c.569G>A, p.Arg190Gln) had been described previously [(13), Table I; supplementary Figure S1 is available at *Mutagenesis* Online]. All the mutations were located in the highly conserved Runt domain.

The R225L (p.Arg225Leu) mutation was a familial one which affected three family members of the Patient 2 (Figure 1A). This mutation was passed on from the affected father to the daughter. Though the three family members shared the same genotype, their phenotype varied dramatically. Supernumerary teeth are usually considered to be a diagnostic feature of CCD, but the expressivity of supernumerary teeth in this family had a striking variation. Panoramic radiograph showed no supernumerary teeth exist in Patient 2 (Figure 2A). However, her young brother was hypodontic (absence of the two mandibular second premolars, Figure 2B), while her father had one supernumerary tooth in the mandibular anterior area

Table I. Clinical and molecular features of the CCD patients in this study

Patient	Family history	Sex (F/M)	Clinical form of CCD	Age (years)	Dental anomalies	Stature (cm)	Mutation				Reference
							Nucleotide[a]	Codon	Type	Location	
1	−	F	Classic	16	++	160	599C>T	T200I	Missense	Runt	This study
2	+	F	Classic	16	+	155	674G>T	R225L	Missense	Runt	This study
3	−	M	Classic	15	++	152	644delG	214fs	Frameshift	Runt	This study
4	−	M	Classic	19	++	157	569G>A	R190Q	Missense	Runt	Zhou *et al.* (13)
5	+	M	Classic	10	++	140	514delT	172fs	Frameshift	Runt	This study
6	+	F	Classic	13	+	163	—	—	—	—	This study

F, female; M, male; $^+$, delayed eruption of permanent teeth; ++, supernumerary teeth and delayed eruption of permanent teeth.
[a]Numbering is based on the 521 as isoform starting with Met Ala Ser Asn Ser.

Downloaded from mutage.oxfordjournals.org at Peking University on September 26, 2010

(Figure 2C). In addition, the severity of hypoplastic clavicles also had an obvious variation among the family members. Bilateral clavicles of the proband were aplasic (Figure 2D), while for her brother (Figure 2E) and father (Figure 2F), the bilateral clavicles were hypoplastic. Besides, chest radiograph of the proband's brother showed scoliosis and spina bifida (Figure 2E).

Frameshift mutation

Two novel frameshift mutations were identified in two male patients and each resulted in premature termination in the Runt domain. One mutation was a single-base deletion (c.644delG, p.His214fs) that was found in a sporadic case, and the other (c.514delT, p.Ser172fs) was familial (Table I; supplementary Figure S1 is available at *Mutagenesis* Online). Both mutations were associated with classic CCD phenotype.

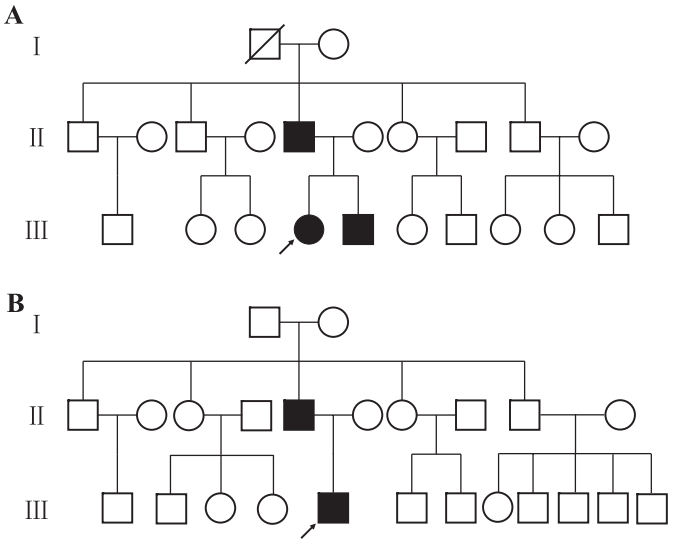

Fig. 1. Pedigree of the family of Patient 2 (**A**) and Patient 5 (**B**). The arrow indicates the proband in each family.

The 172fs (p.Ser172fs) mutation was passed on from the affected father to the son (Figure 1B). Though both of the two patients in this family showed classic CCD phenotypes, craniofacial abnormal appearance of the father was more severe than the proband. Radiograph of the skulls showed patent frontal fontanelles and multiple Wormian bones in the lambdoid and sagittal sutures in both patients (Figure 3). Otherwise, radiograph of the proband's father also presented patent posterior fontanelle, deflection of nasal septum and midface hypoplasia (Figure 3C and D).

Polymorphism

A polymorphism (rs6921145:240G>A, p.A80A, allele frequency: 0.095) was identified on one allele in Patient 1 (supplementary Figure S1 is available at *Mutagenesis* Online), whose healthy mother also carried the transition on one allele. That was an A to G silent transition within the Q/A domain at nucleotide 240.

Subcellular localisation of the RUNX2 mutants

RUNX proteins, in general, have an NLS at the C-terminal border of the Runt domain. Since NLS is necessary for accumulation of RUNX2 protein in the nucleus, it was supposed that mutations that deleted NLS or located in the NLS might affect the subcellular distribution of RUNX2, while mutations out of NLS in Runt domain might have no effect on subcellular location of this protein.

To test this hypothesis, we constructed RUNX2 fusion protein with green fluorescent protein (GFP) tag at the C-terminus in pEGFP-N1 vector. The constructs were transiently transfected into HEK-293A cells. In contrast to GFP control, which was evenly distributed throughout cytoplasm and nucleus (Figure 4A), wild-type RUNX2–GFP fusion protein was detected exclusively in the nucleus (Figure 4B). When isoleucine was substituted for threonine (p.Thr200Ile, T200I), mutant protein showed a similar intracellular distribution with the wild-type RUNX2 (Figure 4C). Thus, T200I mutation did not affect the subcellular location of RUNX2. In contrast, all

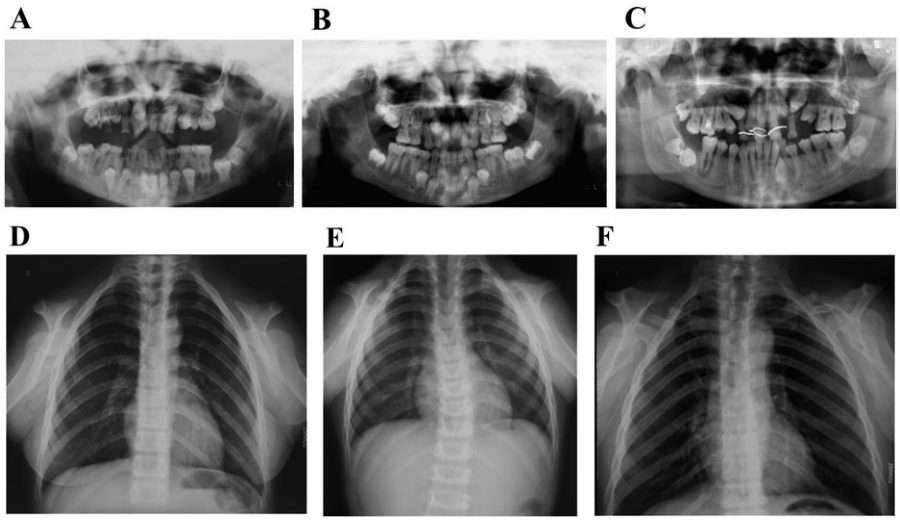

Fig. 2. Radiographic findings in the family members of Patient 2. (**A**) Panoramic radiograph of the proband shows retained deciduous teeth and delayed eruption of permanent teeth. (**B**) Panoramic radiograph of the proband's younger brother shows retained deciduous teeth, delayed eruption of permanent teeth and the absence of the two mandibular second premolars. (**C**) Panoramic radiograph of the proband's father shows one supernumerary tooth in the mandibular anterior area besides typical dental anomalies. (**D**) Chest radiograph of the proband shows bilateral aplasia of clavicles. (**E**) Chest radiograph of the proband's younger brother shows bilateral hypoplasia clavicles, scoliosis and spina bifida. (**F**) Chest radiograph of the proband's father shows bilateral hypoplasia clavicles and pseudarthrosis formation in the right clavicle.

Downloaded from mutage.oxfordjournals.org at Peking University on September 26, 2010

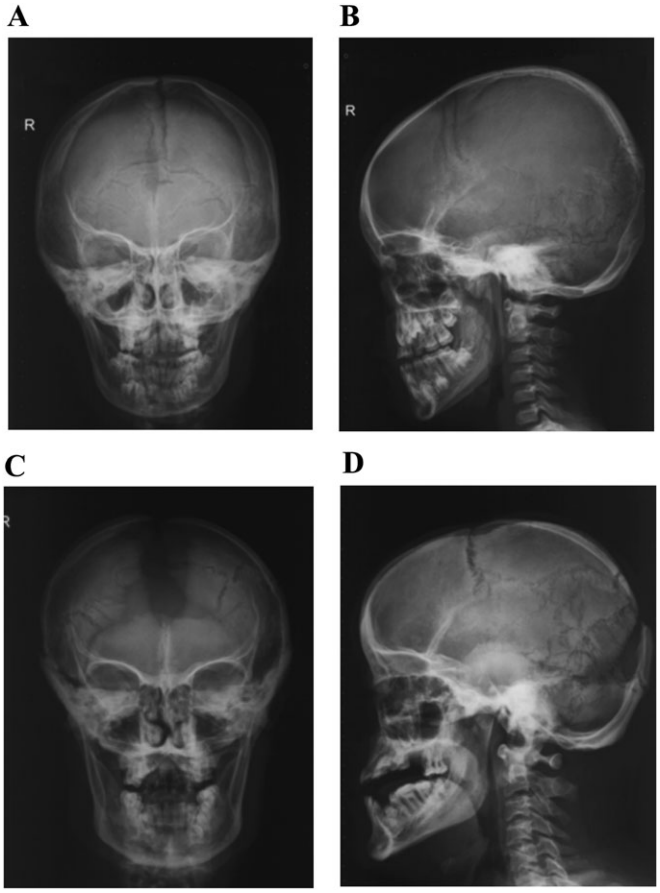

Fig. 3. Radiographic findings in Patient 5 and his father. (**A**) Anteroposterior and (**B**) lateral radiographs of the skull of Patient 5 show patent frontal fontanelle and multiple Wormian bones in the lambdoid and sagittal sutures. (**C**) Anteroposterior and (**D**) lateral radiographs of the skull of the proband's father present patent frontal fontanelle and posterior fontanelle, multiple Wormian bones, deflection of nasal septum and midface hypoplasia.

the three mutants that impaired NLS had an obviously different subcellular location with the wild-type RUNX2–GFP fusion protein. These RUNX2 mutants were unable to quantitatively accumulate in the nucleus. These mutants were R225L mutant (Figure 4D), 214fs (p.His214fs) mutant (Figure 4E) and 172fs mutant (Figure 4F), respectively. Besides located in the nucleus, all the three mutated RUNX2–GFP fusion proteins could also be distributed in the cytoplasm. Thus, mutations that deleted NLS or located in the NLS completely abolished the function of the NLS in accumulating RUNX2 in the nucleus.

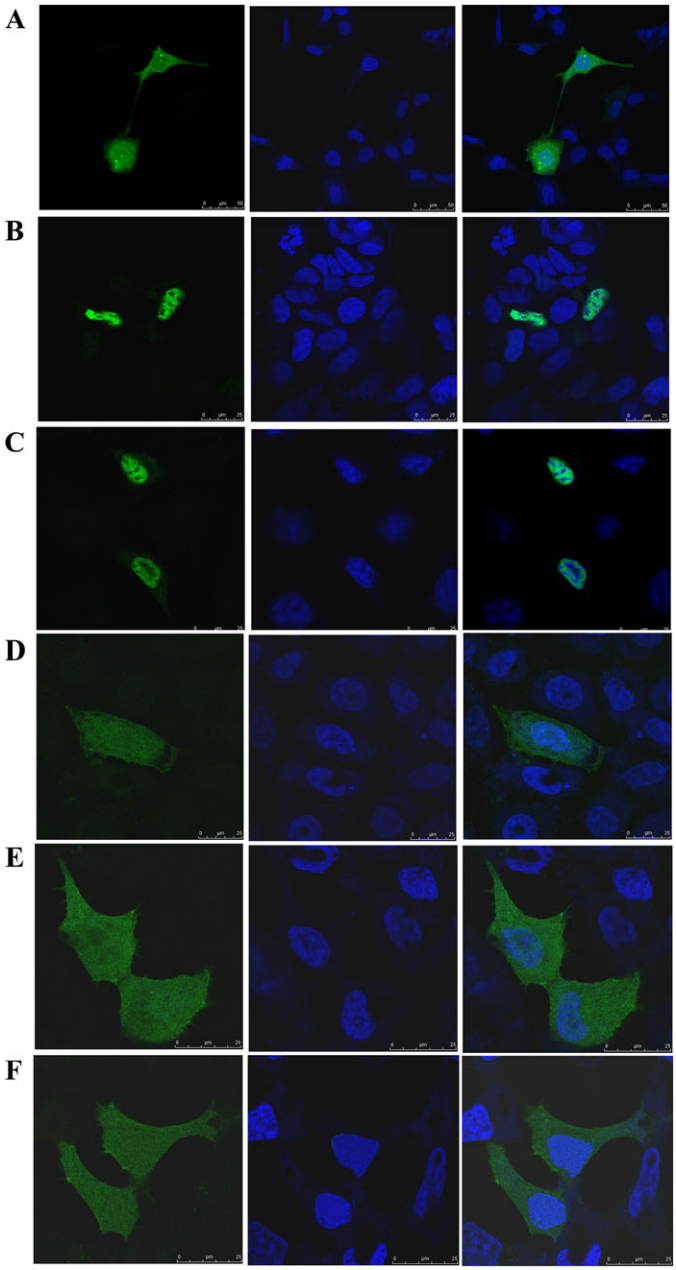

Fig. 4. Subcellular localisation of mutant RUNX2–GFP fusion protein in 293A cells. Confocal micrographs show the intracellular distribution of control GFP (**A**), wild-type RUNX2 (**B**), T200I (**C**), R225L (**D**), 214fs (**E**) and 172fs (**F**) mutant RUNX2 proteins.

Discussion

In the present study, we have identified five different mutations and an additional polymorphism in *RUNX2* gene in six unrelated Chinese CCD patients. Of these mutations, four were novel and one had previously been reported by other study (13).

Our current studies showed that all the five detected mutations were exclusively clustered within the Runt domain. They either directly substituted conserved amino acid residues or caused frameshift and premature termination within this domain. This extreme bias in the distribution of these mutations indicates that the function of the Runt domain with its highly conserved sequence is very susceptible to amino acid changes. Our previous study also indicated that mutations located in the Runt domain severely impaired the trans-activation activities of RUNX2 on the downstream target gene (19). The observed mutational effects on the function of Runt domain are consistent with the information provided by nuclear magnetic resonance and X-ray crystallographic analyses of the Runt domain (20–22).

The NLS is a short basic stretch of nine amino acids that are immediately carboxyl-terminal to the Runt domain [amino acids 221–229 in RUNX2 (VDGPREPRR)] (23,24). And NLS is thought to be responsible for nuclear localisation of RUNX2 protein. The R225 residue is located in this motif, while T200 residue just out of it. 214fs mutation resulted in a frameshift from codon 214 to the resultant premature stop codon 221, leading to a truncated RUNX2 protein at a length of 220 amino

Downloaded from mutage.oxfordjournals.org at Peking University on September 26, 2010

acids. Likewise, the 172fs mutation also brought about a truncated RUNX2 protein at a length of 174 amino acids. Consequently, both of the two frameshift mutations caused the deletion of the NLS. Therefore, it is presumed that R225L, 214fs and 172fs mutations probably affect the subcellular distribution of RUNX2, while mutations out of NLS might have no effect on subcellular location of this protein. To test this hypothesis, we analysed the subcellular distribution of RUNX2–GFP fusion proteins after transient transfection into 293A cells. Distribution of the green fluorescence indicated that all the three mutations—R225L, 214fs and 172fs—completely abolished the function of the NLS, rendering the protein unable to quantitatively accumulate in the nucleus. Overall, these results are consistent with the previous proposal that a lack of nuclear RUNX2 accumulation is the cause of haploinsufficiency in these cases (2,17). Though T200I mutation did not affect the subcellular distribution of RUNX2, this missense mutation was also located in the Runt domain and severely impaired the transactivation activity of RUNX2 on the downstream target gene in our reporter gene assay (19). And this is consistent with previous study about the mutation effect of the T200A mutation (13). Thus, impaired transactivation activity of RUNX2 might be the potential reason why this kind of patients showed typical CCD phenotype.

In our patient cohort, though all the patients displayed classic CCD phenotypes with hypoplastic clavicles, delayed closure of the fontanelle and dental abnormalities, there is a wide range of clinical expressivity of phenotype, even among family members. The phenotypic diversity of our CCD patients confirms the known CCD phenotypic variability (1). The occurrence of intrafamilial clinical variability suggests that hypomorphic effects and genetic modifiers may alter the clinical expressivity of these mutations, and the most likely modifier may be the transcriptional level of the remaining unaffected allele. The hypomorphic effects being the cause of CCD phenotypic variability was proved by a homozygous *RUNX2*$^{neo7/neo7}$ mice model, which expressed a reduced level of wild-type *RUNX2* mRNA (55–70%) and protein and appeared CCD phenotype (25). Thus, the range of bone phenotypes in CCD patients may be associated with quantitative reduction in the functional activity of *RUNX2*.

Supernumerary teeth are usually considered to be a diagnostic feature of CCD. However, the expressivity of supernumerary teeth in our patient cohort had a striking variation, even among family members. There was no supernumerary tooth existing in two female patients, while 11 supernumerary teeth existed in a male patient (Patient 4, data not shown). Besides, the young brother of Patient 2 was hypodontic (Figure 3B), while her father had one supernumerary tooth in the mandibular anterior area (Figure 3C). All the expressivity variation of supernumerary teeth in our patient cohort is consistent with previously reports (26,27). In addition, we also found a slight relationship between the numbers of supernumerary teeth and body height of the male patients as previously reported (28).

In the present study, no mutation was identified in one familial case. The possible reason is that partial gene deletions, intronic variations or regulatory changes can also impair RUNX2 expression besides intragenic point mutations. In addition, chromosome abnormality or intragenic microdeletion of RUNX2 was demonstrated to be another mechanism for CCD (29,30). Further analysis will be required to answer these questions.

Supplementary data

Supplementary Figure S1 is available at *Mutagenesis* online.

Funding

Beijing Municipal Natural Science Foundation, People's Republic of China (7092112).

Acknowledgements

We are grateful to all the patients and their family members for their participation and contributions. We are grateful to Dr Renny T. Franceschi (School of Dentistry, University of Michigan), Dr T. J. Li (Department of Oral Pathology, Peking University School and Hospital of Stomatology) and Dr Y. H. Gan (Research Laboratory of Oral and Maxillofacial Surgery, Peking University School and Hospital of Stomatology) for providing *Runx2* cDNA, HEK-293A cells and pEGFP-N1 vector respectively.

Conflict of interest statement: None declared.

References

1. Mundlos, S. (1999) Cleidocranial dysplasia: clinical and molecular genetics. *J. Med. Genet.*, **36**, 177–182.
2. Quack, I., Vonderstrass, B., Stock, M., Aylsworth, A. S., Becker, A., Brueton, L. *et al.* (1999) Mutation analysis of core binding factor A1 in patients with cleidocranial dysplasia. *Am. J. Hum. Genet.*, **65**, 1268–1278.
3. Otto, F., Kanegane, H. and Mundlos, S. (2002) Mutations in the RUNX2 gene in patients with cleidocranial dysplasia. *Hum. Mutat.*, **19**, 209–216.
4. Lee, B., Thirunavukkarasu, K., Zhou, L., Pastore, L., Baldini, A., Hecht, J. *et al.* (1997) Missense mutations abolishing DNA binding of the osteoblast-specific transcription factor OSF2/CBFA1 in cleidocranial dysplasia. *Nat. Genet.*, **16**, 307–310.
5. Mundlos, S., Otto, F., Mundlos, C., Mulliken, J. B., Aylsworth, A. S., Albright, S. *et al.* (1997) Mutations involving the transcription factor CBFA1 cause cleidocranial dysplasia. *Cell*, **89**, 773–779.
6. Otto, F., Thornell, A. P., Crompton, T., Denzel, A., Gilmour, K. C., Rosewell, I. R. *et al.* (1997) Cbfa1, a candidate gene for cleidocranial dysplasia syndrome, is essential for osteoblast differentiation and bone development. *Cell*, **89**, 765–771.
7. Komori, T., Yagi, H., Nomura, S., Yamaguchi, A., Sasaki, K., Deguchi, K. *et al.* (1997) Targeted disruption of Cbfa1 results in a complete lack of boneformation owing to maturational arrest of osteoblasts. *Cell*, **89**, 755–764.
8. Huang, L. F., Fukai, N., Selby, P. B., Olsen, B. R. and Mundlos, S. (1997) Mouse clavicular development: analysis of wild-type and cleidocranial dysplasia mutant mice. *Dev. Dyn.*, **210**, 33–40.
9. Ogawa, E., Maruyama, M., Kagoshima, H., Inuzuka, M., Lu, J., Satake, M. *et al.* (1993) PEBP2/PEA2 represents a new family of transcription factor homologous to the products of the Drosophila *runt* and the human *AML1* gene. *Proc. Natl Acad. Sci. USA*, **90**, 6859–6863.
10. Gutierrez, S., Javed, A., Tennant, D. K., van Rees, M., Montecino, M., Stein, G. S. *et al.* (2002) CCAAT/enhancer-binding proteins (C/EBP) beta and delta activate osteocalcin gene transcription and synergize with Runx2 at the C/EBP element to regulate bone-specific expression. *J. Biol. Chem.*, **277**, 1316–1323.
11. Lian, J. B., Javed, A., Zaidi, S. K., Lengner, C., Montecino, M., van Wijnen, A. J. *et al.* (2004) Regulatory controls for osteoblast growth and differentiation: role of Runx/Cbfa/AML factors. *Crit. Rev. Eukaryot. Gene Expr.*, **14**, 1–42.
12. Zaidi, S. K., Young, D. W., Choi, J. Y., Pratap, J., Javed, A., Montecino, M. *et al.* (2005) The dynamic organization of gene-regulatory machinery in nuclear microenvironments. *EMBO Rep.*, **6**, 128–133.
13. Zhou, G., Chen, Y., Zhou, L., Thirunavukkarasu, K., Hecht, J., Chitayat, D. *et al.* (1999) CBFA1 mutation analysis and functional correlation with phenotypic variability in cleidocranial dysplasia. *Hum. Mol. Genet.*, **8**, 2311–2316.
14. Tessa, A., Salvi, S., Casali, C., Garavelli, L., Digilio, M. C., Dotti, M. T. *et al.* (2003) Six novel mutations of the *RUNX2* gene in Italian patients with cleidocranial dysplasia. *Hum. Mutat.*, **22**, 104–109.
15. Xuan, D., Li, S., Zhang, X., Hu, F., Lin, L., Wang, C. *et al.* (2008) Mutations in the RUNX2 gene in Chinese patients with cleidocranial dysplasia. *Ann. Clin. Lab. Sci.*, **38**, 15–24.

Downloaded from mutage.oxfordjournals.org at Peking University on September 26, 2010

16. Li, Y. L., Pan, W., Xu, W. F., He, N., Chen, X. W., Liu, H. *et al.* (2009) RUNX2 mutations in Chinese patients with cleidocranial dysplasia. *Mutagenesis*, **24**, 425–431.
17. Yoshida, T., Kanegane, H., Osato, M., Yanagida, M., Miyawaki, T., Ito, Y. *et al.* (2002) Functional analysis of *RUNX2* mutations in Japanese patients with cleidocranial dysplasia demonstrates novel genotype-phenotype correlations. *Am. J. Hum. Genet.*, **71**, 724–738.
18. Puppin, C., Pellizzari, L., Fabbro, D., Fogolari, F., Tell, G., Tessa, A. *et al.* (2005) Functional analysis of a novel RUNX2 missense mutation found in a family with cleidocranial dysplasia. *J. Hum. Genet.*, **50**, 679–683.
19. Zhang, C. Y., Zheng, S. G., Wang, Y. X., Zhu, J. X., Zhu, X., Zhao, Y. M. *et al.* (2009) Novel *RUNX2* mutations in Chinese individuals with cleidocranial dysplasia. *J. Dent. Res.*, **88**, 861–866.
20. Bravo, J., Li, Z., Speck, N. A. and Warren, A. J. (2001) The leukemia-associated AML1 (Runx1)–CBFb complex functions as a DNA-induced molecular clamp. *Nat. Struct. Biol.*, **8**, 371–378.
21. Tahirov, T. H., Inoue-Bungo, T., Morii, H., Fujikawa, A., Sasaki, M., Kimura, K. *et al.* (2001) Structural analyses of DNA recognition by the AML1/Runx-1 Runt domain and its allosteric control by CBFb. *Cell*, **104**, 755–767.
22. Nagata, T. and Werner, M. H. (2001) Functional mutagenesis of AML1/RUNX1 and PEBP2b/CBFb define distinct, non-overlapping sites for DNA recognition and heterodimerization by the Runt domain. *J. Mol. Biol.*, **308**, 191–203.
23. Kanno, T., Kanno, Y., Chen, L. F., Ogawa, E., Kim, W. Y. and Ito, Y. (1998) Intrinsic transcriptional activation-inhibition domains of the polyomavirus enhancer binding protein 2/core binding factor alpha subunit revealed in the presence of the beta subunit. *Mol. Cell. Biol.*, **18**, 2444–2454.
24. Thirunavukkarasu, K., Magajaan, M., McLarren, K. W., Stifani, S. and Karsenty, G. (1998) Two domains unique to osteoblast-specific transcription factor Osf2/Cbfa1 contribute to its transactivation function and its inability to heterodimerize with Cbfb. *Mol. Cell. Biol.*, **18**, 4197–4208.
25. Lou, Y., Javed, A., Hussain, S., Colby, J., Frederick, D., Pratap, J. *et al.* (2009) A Runx2 threshold for the cleidocranial dysplasia phenotype. *Hum. Mol. Genet.*, **18**, 556–568.
26. Hardt, N. (1973) Osteo-dental dysplasia with poly- and hypodontia in cleidocranial dysostosis. *Quintessenz*, **24**, 105–111.
27. Baumert, U., Golan, I., Redlich, M., Aknin, J. J. and Muessig, D. (2005) Cleidocranial dysplasia: molecular genetic analysis and phenotypic-based description of a Middle European patient group. *Am. J. Med. Genet.*, **139**, 78–85.
28. Yoshida, T., Kanegane, H., Osato, M., Yanagida, M., Miyawaki, T., Ito, Y. *et al.* (2003) Functional analysis of *RUNX2* mutations in cleidocranial dysplasia: novel insights into genotypephenotype correlations. *Blood Cells Mol. Dis.*, **30**, 184–193.
29. Izumi, K., Yahagi, N., Fujii, Y., Higuchi, M., Kosaki, R., Naito, Y. *et al.* (2006) Cleidocranial dysplasia plus vascular anomalies with 6p21.2 microdeletion spanning RUNX2 and VEGF. *Am. J. Med. Genet. A*, **140**, 398–401.
30. Lee, M. T., Tsai, A. C., Chou, C. H., Sun, F. M., Huang, L. C., Yin, P. L. *et al.* (2008) Intragenic microdeletion of RUNX2 is a novel mechanism for cleidocranial dysplasia. *Genomic Med.*, **2**, 45–49.

Downloaded from mutage.oxfordjournals.org at Peking University on September 26, 2010